

**Design, Fabrication, and Testing
of a
Composite Rack Prototype
in support of the
Deep Space Habitat Program**

Russ Smith & Richard Hagen

Abstract

In support of the Deep Space Habitat project a number of composite rack prototypes were developed, designed, fabricated and tested to various extents (with the International Standard Payload Rack configuration, or crew quarters, as a baseline) . This paper focuses specifically on a composite rack prototype with a direct tie in to Space Station hardware. The outlined prototype is an all composite construction, excluding metallic fasteners, washers, and their associated inserts. The rack utilizes braided carbon composite tubing for the frame with the sidewalls, backwall and flooring sections utilizing aircraft grade composite honeycomb sandwich panels. Novel additively manufactured thermoplastic joints and tube inserts were also developed in support of this effort. Joint and tube insert screening tests were conducted at a preliminary level. The screening tests allowed for modification, and enhancement, of the fabrication and design approaches, which will be outlined. The initial joint tests did not include mechanical fasteners. Adhesives were utilized at the joint to composite tube interfaces, along with mechanical fasteners during final fabrication (thus creating a stronger joint than the adhesive only variant). In general the prototype was focused on a potential in-space assembly approach, or kit-of-parts construction concept, which would not necessarily require the inclusion of an adhesive in the joint regions. However, given the tie in to legacy Station hardware (and potential flight loads with imbedded hardware mass loadings), the rack was built as stiff and strong as possible. Preliminary torque down tests were also conducted to determine the feasibility of mounting the composite honeycomb panels to the composite tubing sections via the additively manufactured tube inserts. Additional fastener torque down tests were also conducted with inserts (helicoils) imbedded within the joints. Lessons learned are also included and discussed.

Introduction

In support of the Deep Space Habitat (DSH) Program, a Composite Rack (CR) prototype has been designed and fabricated with selective testing of specific joining features. The design utilized the International Standard Payload Rack (ISPR) as the baseline (which is prominent on ISS) and which can be seen in Figure 1. An all metallic prototype concept, comprised of commercial off the shelf (COTS) components, and which utilized extruded aluminum beam sections for the frame, as well as aluminum honeycomb panels, preceded the currently outlined CR and also helped to form a point of departure based upon legacy Station ISPRs, or crew quarters (Ref 1).

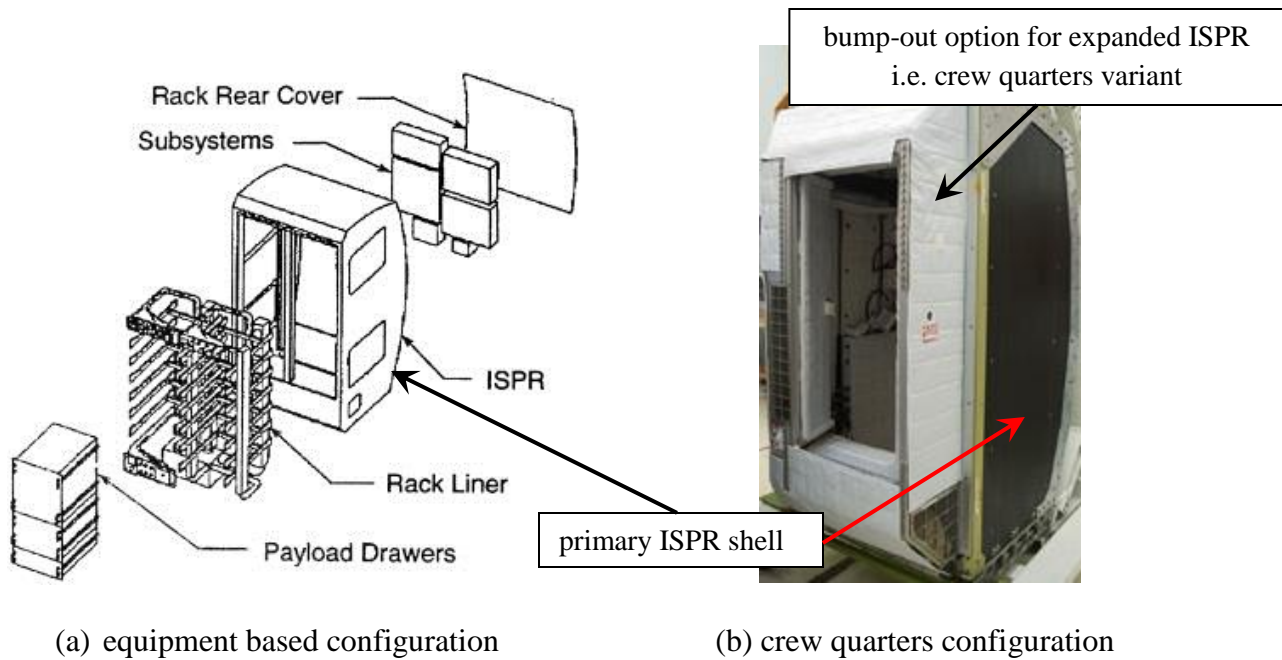


Figure 1. Two ISPR variants

A textile based Inflatable/Deployable Evolved ISPR (or IDE-I), is currently being investigated in a joint effort with the Navy/NAVSEA in Newport, RI and which will conclude the series of prototyping associated with metallic, composite, and inflatable/fabric based secondary structures (Ref. 1). However, it should be noted that a flight loads spectrum response was not investigated for these concept prototypes given resource availability. By exploring the use of composite structures, combined with additively manufactured components, as well as novel assembly methods and materials, there is a potential for weight savings as compared to more traditional approaches. Given in-space assembly feasibility, significant weight savings could be achieved for the various rack prototypes because they would no longer have to endure induced launch loads with the mass of mounted internal equipment (whereby those loads are reacted thru the rack frame and joints in current launch scenarios). Typically, ISPRs provide about 55.5 ft³ of volume at a weight of 230lbs with an internal payload carrying capacity of 1540lbs (Ref 2).

The CR was demonstrated during the Marshall Space Flight Center's (MSFC) DSH walk-thru in support of the Lyndon B. Johnson Space Center's (JSC) annual Mission Operations Testing (MOT) activity. The CR was a self-standing unit outside of the actual mockup, where the aforementioned all metallic 8020-FabPro was installed as a Crew Quarters (CQ) inside the Multi-purpose Logistics Module (MPLM). Shown in Figure 2 is the as shipped CR. Assembly techniques demonstrated with the CR could be used to assemble light weight secondary structures after launch, thus avoiding the need for extra structural material to handle launch loads. The weight of the CR was 120 lbs.



(a) left side view

(b) front view

(c) right side view

Figure 2. Various views of the final CR assembly.

Design

Plan form:

Given the short time frame to design and build the CR a simplified profile was developed which reduced the number of joints needed in the rack assembly and also helped reduce fabrication time and production costs. Simplification of the rack profile reduces the volume by only 5.5% (i.e. -3.5 ft^3) which results in a rack volume of approximately 52 ft^3 . The weight of the CR was 120 lbs (dominated by the composite honeycomb panel sections, which were repurposed from a prior DSH effort). Shown in Figure 3 is the simplified reduced plan-form profile in green with the original profile in blue for comparison purposes. The gap on the backside of the rack could be utilized for additional logistics (i.e. cooling lines for the equipment, electrical conduits, etc..) or even as possible storage space for inflatable/deployable secondary structures.

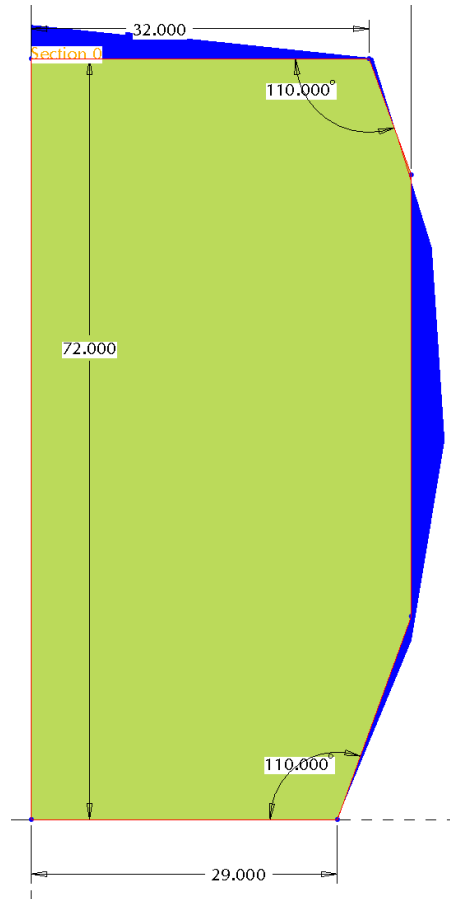


Figure 3. CR profile overlaid on the original ISPR profile (units in inches).

Frame Tubing and Panel Sections:

Initially, utilizing a high grade fiberglass material such as G10 was envisioned as the basic frame tube stock. However, G10 is relatively dense (and thus heavy), and it was decided that lighter and more state-of-the-art (SoA) type composite tubing should be investigated as part of this effort. As a result, braided carbon fiber/epoxy tubing was selected as shown in Figure 4.

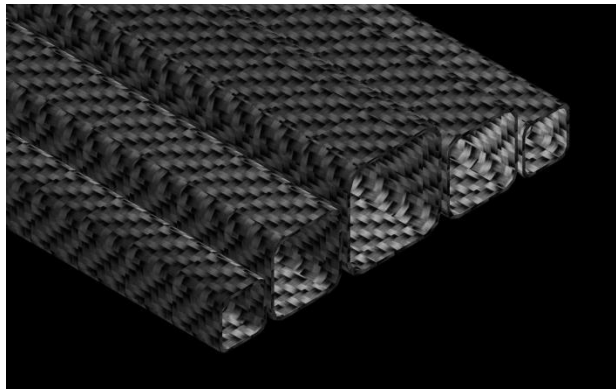


Figure 4. Braided carbon-fiber composite tubing.

The braided carbon fiber tubing and uni-directional fabric construction allows for light weight framing and is designed to be stronger in bending, and torsion (say than pultruded equivalents), and is also lighter. The unidirectional fabric sections are sandwiched within the braided layers, which greatly reduces the potential for longitudinal crack propagation (Ref 3). The tubing is 2 inches by 2 inches nominal, with a wall thickness of approximately 65 mils, and which weighs 0.26 lbs/ft.

Due to the rapid prototyping nature of this effort aircraft grade cargo flooring was utilized for the CR wall sections (Ref 4). Shown in Figure 5 are several representative layers of the honeycomb composite panels. Only a single panel layer was used for the side walls, back clam shell and flooring. The core section consisted of 1/8th inch cell size Nomex, at 9 lbs/ft³, and which was 0.66 inches thick. The facesheets had 3 plies each, with a thickness of 0.010 inches per ply, made from woven E-glass with epoxy reinforcement. Both four point bending tests and core crush tests were conducted as part of the previous research effort (see Ref 4) with a nominal compressive strength around 1,800 psi (as verified by testing).



Figure 5. Honeycomb composite panels utilized in design.

Joints, Inserts and Attachments:

A joint prototype effort was initiated at the beginning of this research with the trimetric joints of the composite rack being fabricated via the fused deposition modeling (FDM) process. The FDM process is one of many additive manufacturing (AM) approaches which have gained great popularity over the last few years due to its ability to produce final net parts at minimal costs. Additionally, this method of manufacturing proved to be cost effective due to the low number of joints needed and machine availability. Also, by using a FDM process over a traditionally machined part, a 0.25 pound weight savings per joint was achieved. Greater weight savings could be achieved with additional analysis and testing. The FDM process is currently the leading AM process for use in a reduced gravity environment.

Given the applicability of the AM approach to space habitats (i.e. in-space assembly and manufacturing), a sequence of qualifying flight experiments would be warranted address issues associated with a micro-gravity environment (no natural convective heat transfer and the need for an iso-thermal environment for the part as it is produced). Currently the University of Wisconsin is working on such a prototype as part of NASA's X-Hab educational outreach activity (Ref 5). Additionally, the Made In Space company will be flying a limited FDM type printer which is slated for delivery to ISS in 2014 (Ref 6).

Shown in Figure 6 is the first joint concept prototype developed and which had the root base block (red colored) as a solid cube which was 2 inches on a side (i.e. 2 in^3), the white wall thicknesses were $\frac{1}{4}$ inch and the green base wall thicknesses were 0.185 inches. Also included is an adhesive layer feature (the green strips shown on the white wall sections) which would allow the adhesive layer to be in the 5 mil range while simultaneously helping to center the tube on the joint section.

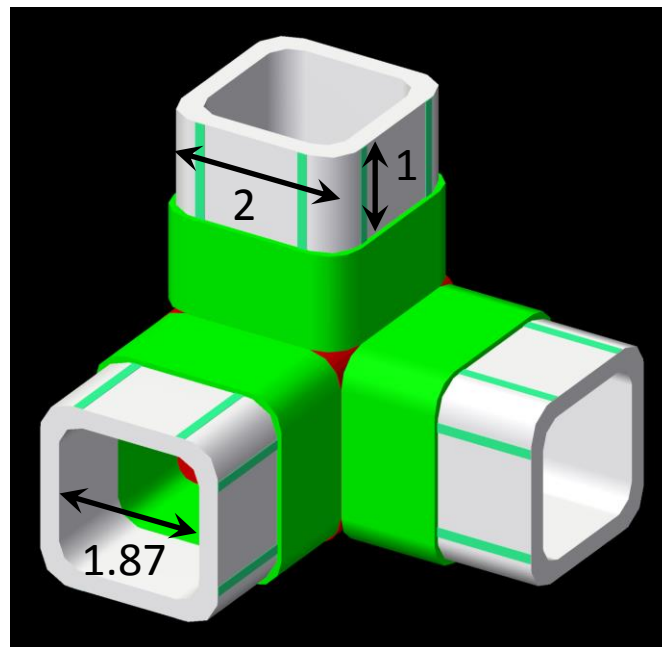


Figure 6. Initial AM/FDM joint prototype (units in inches).

Subsequently it was decided that mechanical attachment features should be added at the joint/tube interfaces and that such sections would need to accommodate 10-32UNF type fasteners (which are widely utilized in commercial aviation). Also, fillets and/or radiuses were added at the joint intersections to help reduce stress concentrations associated with the initial design. Shown in Figure 7 is an intermediate printed joint which extended both the tube/joint interface section, as well as the root collar section, out to 2 inches in extent. This joint prototype weighed 1.18 lbs.

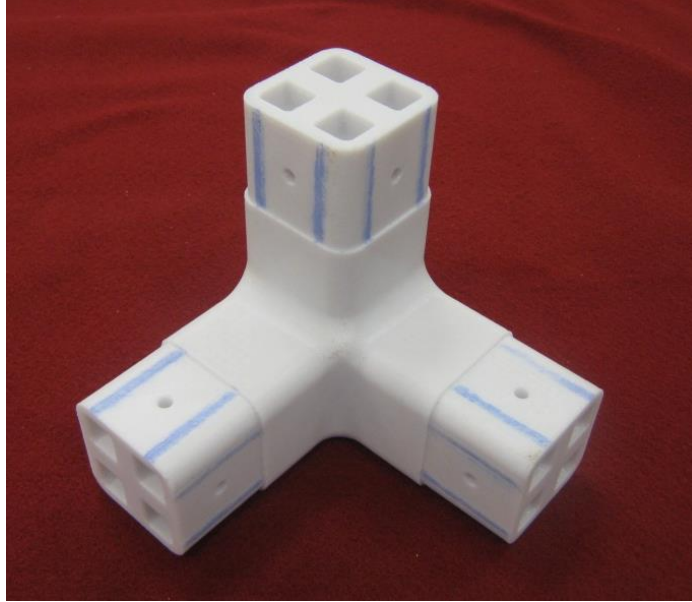
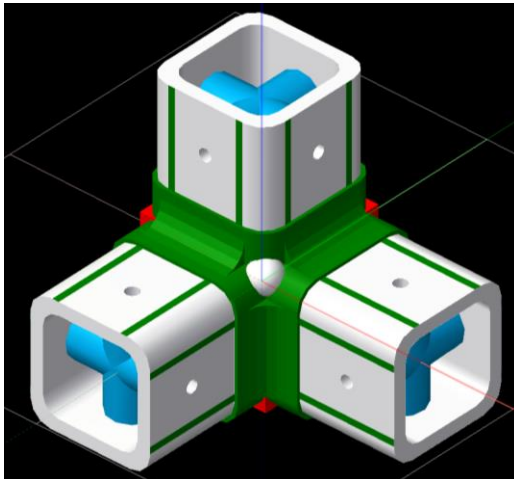
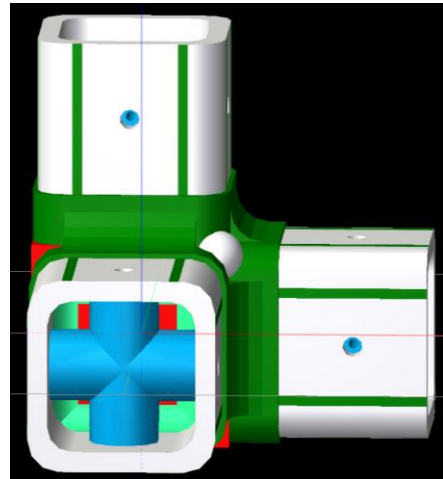


Figure 7. Intermediate AM joint prototype.

Shown in Figure 8 is the second joint prototype design in the series of joints investigated with the interior blue “cross” allowing for an easy installation of the fasteners and which was an outgrowth from the previously detailed intermediate joint design. Note that the base root collar section was shortened towards the joint root cube as a result of the inclusion of the fillet and radius sections. This allowed the adhesive interface section of the joint (i.e. the white tube) to be extended an additional 0.5 inches such that the total adhesive interface area was increased by 50%.



(a) isometric view



(b) interior view

Figure 8. 2nd generation AM joint prototype.

The initial sequence of joint prototypes were designed using VectorWorks2012 (Ref 7), with subsequent versions being designed in CREO Parametric 2.0 (Ref 8). Shown in Figure 9 is the stereo-lithography file (or *.stl), as submitted to the fabrication machine. This joint prototype weighed 0.86 lbs.

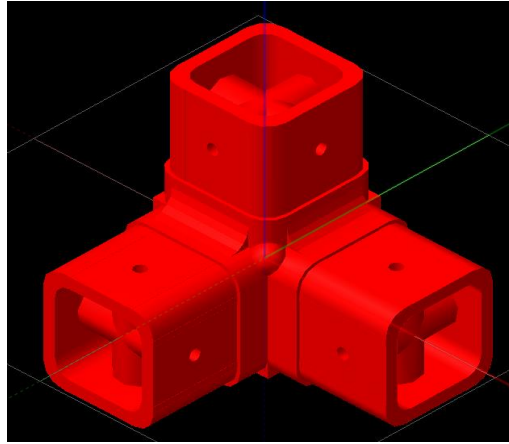
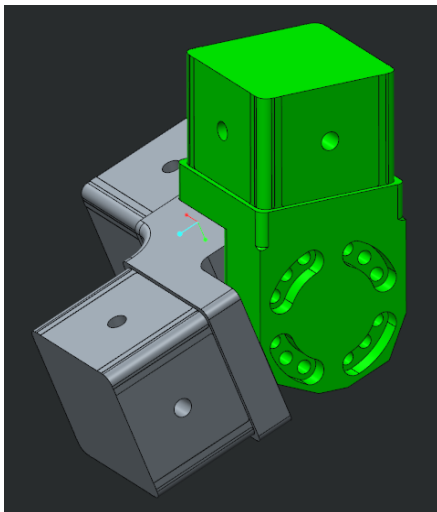
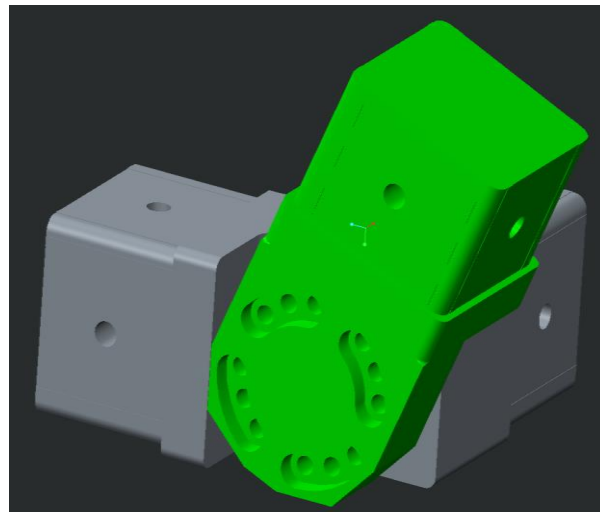


Figure 9. Stereo-lithography file, *.stl, as submitted for printing.

Additional joints were also investigated which included a mechanistic joint prototype as shown in Figure 10. The intent of this design was to have a joint that is used at all intersections and eliminate the need for different joint configurations (i.e. a universal joint). However, after development of the design it was found that it weighed 50% more and cost three times more than the simpler FDM joint. Additionally, there is the added complexity of transferring loads through a bolted joint (load path) and the knock down factors (or factors of safety) associated with such a configuration. Thus, it was determined that a universal mechanistic joint had a much higher risk than the tri-metric designs.



(a) isometric view #1



(b) isometric view #2

Figure 10. 3rd generation AM joint prototype.

The final joint sets are shown in Figure 11. Due to very tight fabrication and delivery schedules, production of the joints, inserts and other components were done concurrently at JSC and LaRC. Additional details of the design and fabrication approach are outlined in the fabrication subsection.

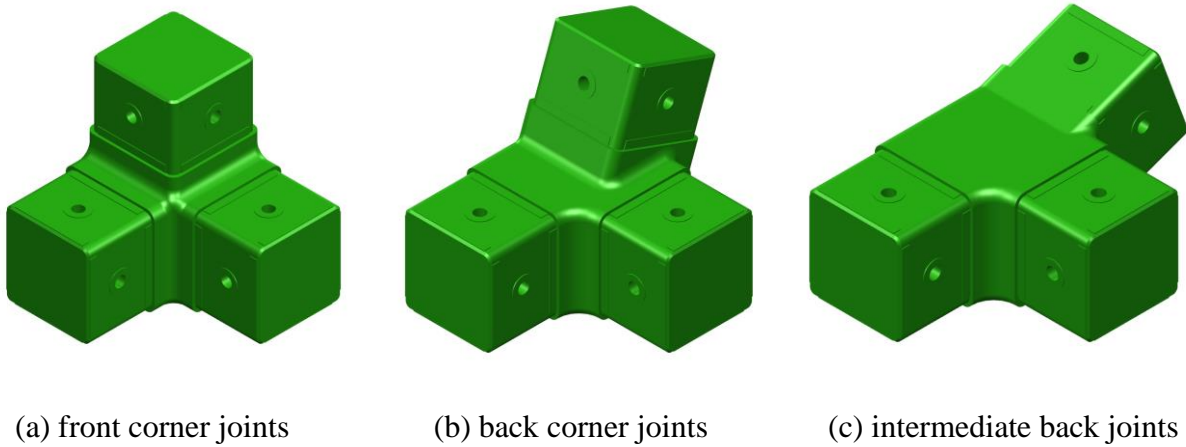
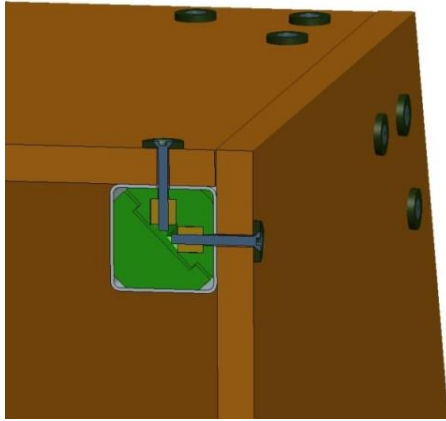


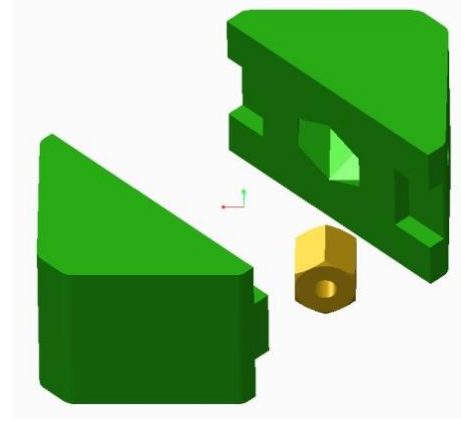
Figure 11. Final trimetric FDM joints (4 each/rack).

Inserts

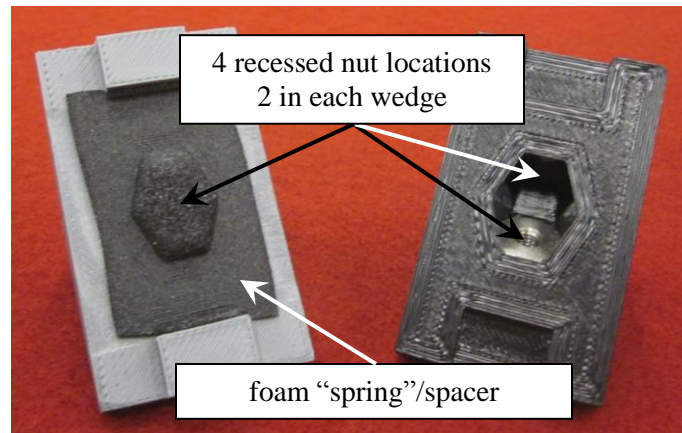
Shown in Figure 12 are computer aided design, or CAD renderings (Ref 8) of the initial composite tube inserts (or 1st generation) as well as the 3D printed part. This was the first iteration of an imbedded tube insert, which has several design features not continued in later iterations; discontinued features were the interlocking tabs on the block sections, the long profile nut and the two nut limit per insert.



(a) tube insert installed in tube/panel



(b) exploded view of insert details



(c) 3D printed part

Figure 12. 1st generation composite tube insert.

After installing the first set of inserts it seemed more advantageous to have four captive nuts instead of two (which would allow for mechanical fasters along every side). Additionally, the captive nuts initially chosen were more expensive than a standard nut, but did not provide a significant improvement. Thus, the second generation composite tube insert (Figure 13) was developed for additional evaluation. However, due to tight delivery schedules, the 1st generation design was installed and worked well.

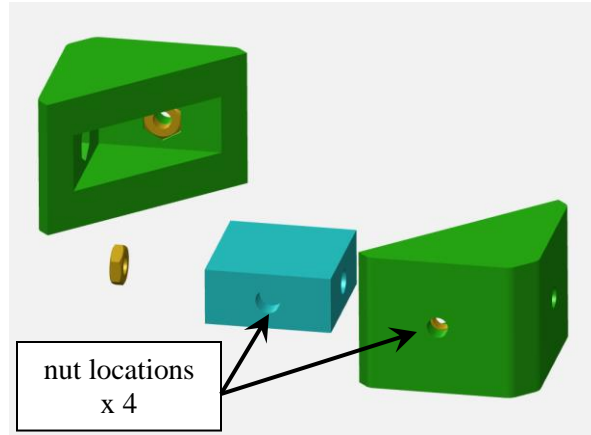
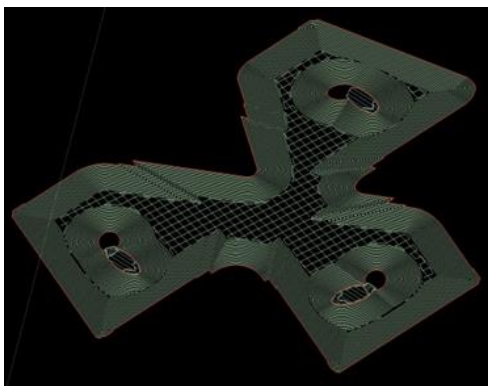


Figure 13. 2nd generation composite tube FDM insert concept.

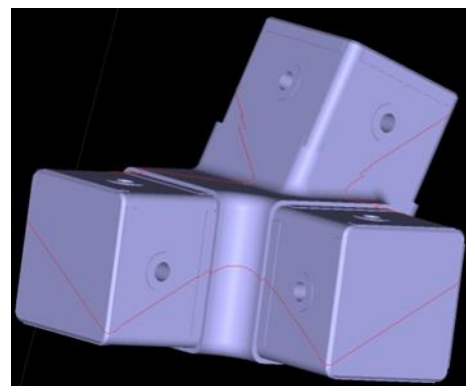
Potentially optimizing the joint design for the FDM process was an additional consideration. The component was made with minimal support needed while in the printing chamber, and also utilizes the sparse fill interior to minimize mass. The sparse fill approach is outlined in more detail in the next section (but which effectively forms an interior honeycomb type structure).

Fabrication

By iterating on the designs and manufacturing approaches a 0.25 pound weight savings per joint was achieved. This was done by adjusting the build orientation (the three dimensional orientation of the piece being built in coordination with the nozzle head, and both its planar and vertical motion) and making the interior of the joint a honeycomb like structure (a.k.a. sparse fill). The authors are confident that additional weight savings could be achieved with additional analysis and testing. Figure 14 shows some of the outlined details, and in particular the honeycomb type, sparse fill interior, as well as the material bead layers, extruded from the nozzle head, which were deposited in 0.010 inch layers (Ref 9).



(a) 0.4 inch wall with honeycomb interior



(b) red line denotes a 0.01 inch thick layer

Figure 14. Joint, with honeycomb sparse interior type fill, and fabrication layering details.

Also, in order to help reduce material anisotropy associated with the fabrication process, and to aid in the principal material directions lining up more with the composite tube structural load paths, the final joints were fabricated at a 45° incline to the machine nozzle head. Shown in Figure 15 is a rendering of one of the front trimetric joints, oriented for structural integrity with fabrication efficiency, and as the part would appear at the end of the FDM printing.

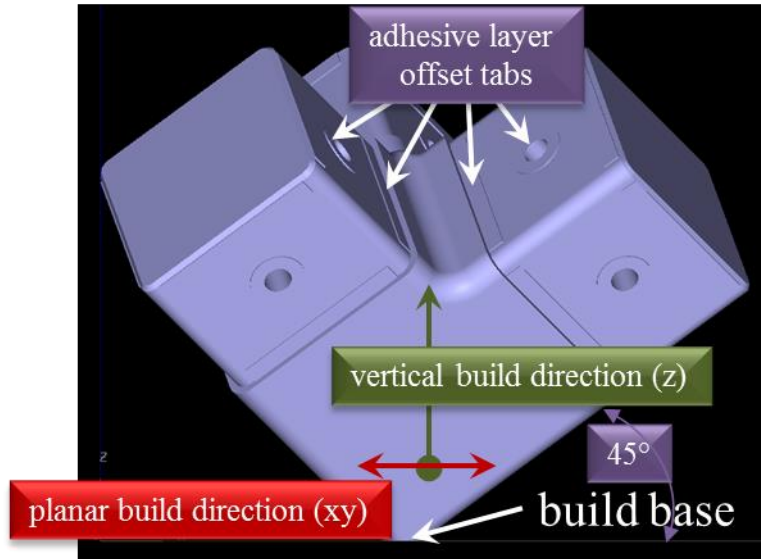


Figure 15. 45° orientation for joint build up with supply head feed (planar motion in-plane, xy, per layer, then vertical motion (z) for the next layer).

All of the pieces manufactured at JSC are shown in Figure 16. Note the grey c-bracket pieces in the back of the figure which were used to support the lower composite hat sections. The hat sections are not shown (there were two), but the hat crowns fed into the c-brackets, with the flanges of the composite hat stiffeners bonded to the bottom surface of the floor section.

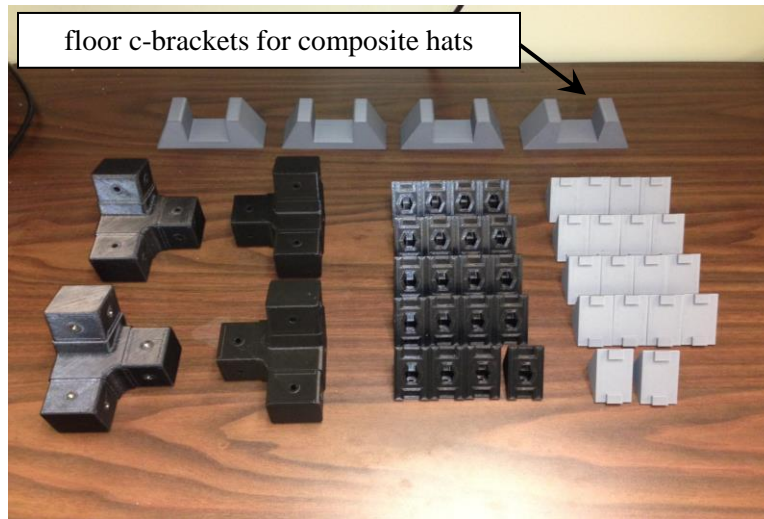
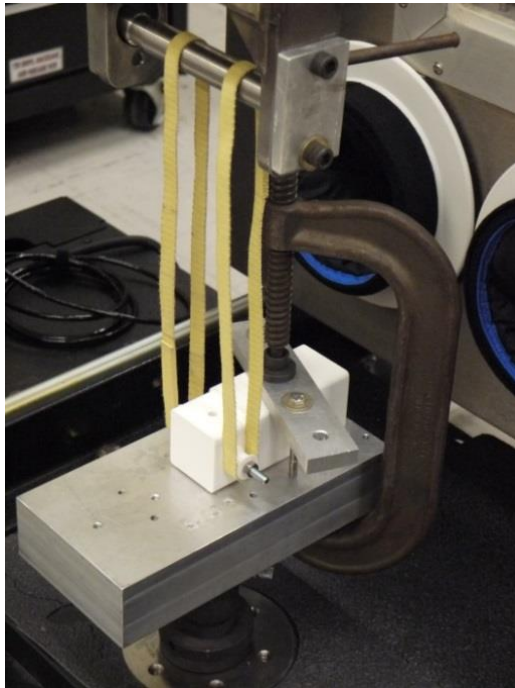


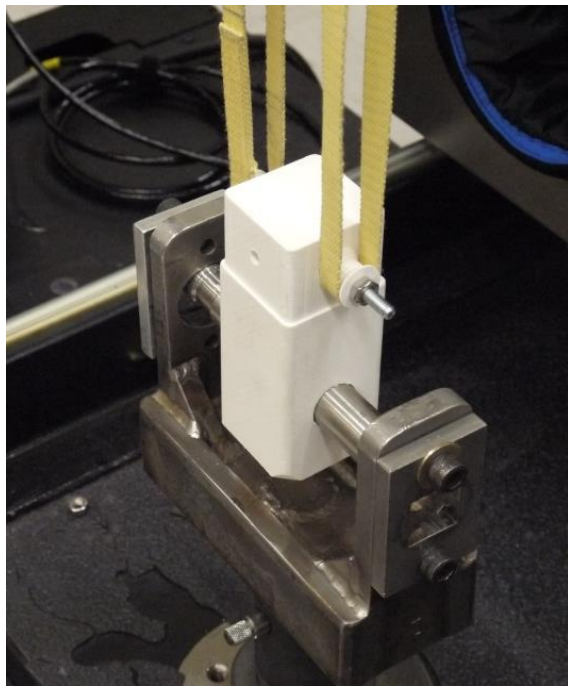
Figure 16. AM components via the Stratasys-Fortus eV machine at JSC.

Testing

Screening test sequences were conducted to help determine the basic joint response, but which subsequently included adhesive joint response/strength assessments as well. The initial joint response test set-ups are shown in Figure 17 which included both a bending test as well as a tensile test. It was initially believed that the failure load of the joint would be below a 2000 lbf ultimate load, but during testing the capacity of the load cell was superseded and the loading pin thru the specimen bent (during the bending test phase). Figure 18 shows the bending response of the specimen with the tensile response shown in Figure 19. It should be noted that in all of the load displacement plots that the raw data is in color, and that the linear curve fit of the data is in black. Additionally, the root mean square linear curve fit is denoted as R^2 , with a perfect straight line having a value of 1.0 (and thus values very close to 1, are very nearly linear). The bending stress response was governed by $\sigma_b = Mc/I$ and tension by $\sigma_t = F/A$. Two test specimens were manufactured in the 45° orientation to reduce anisotropy (i.e. increase isotropy). As shown, Kevlar straps were placed around roller assemblies on each specimen and pulled to 2000 lbf. Included in Appendix A is the raw data along with associated curve fits to account for load pick-up nonlinearities (i.e. load train slop, strap slack, etc.). In the case of the bending response, due to the angled support bar, a mild degree of torsion was also induced, however, the approximate support distance was about 1.75 inches, so at maximum load $\sigma_b \approx 2,625$ psi (tensile and compressive), whereas for the tensile load case $\sigma_t \approx 500$ psi (tension).



(a) bending test



(b) tensile test

Figure 17. Joint response screening experiments.

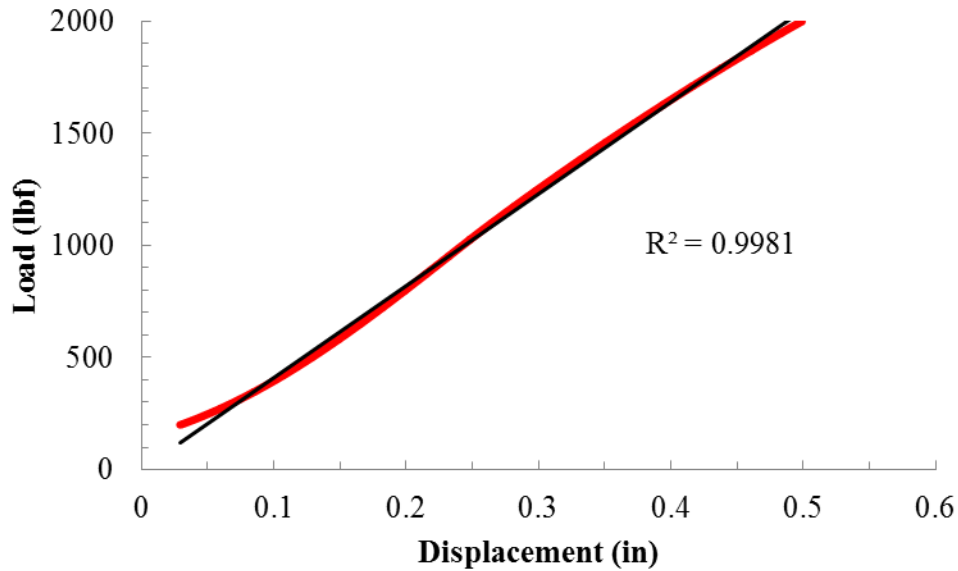


Figure 18. Load vs. displacement bending test.

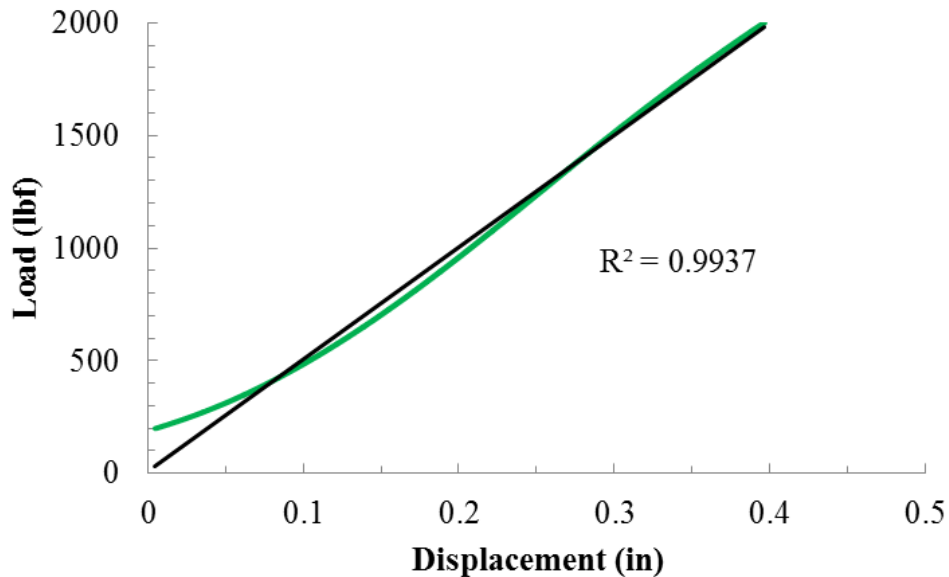


Figure 19. Load vs. displacement tensile test.

Due to the fact that the joints appeared to have good load bearing properties, and the nature of the rapid prototyping effort, it was decided that adhesive joint strength tests would be conducted next, and which accounted for a possible higher load level than the initial value of 2000 lbf.

Shown in Figure 20 is a picture of the refined test set-up; the two different adhesive joints were designed such that one adhesive offset tab ran longitudinal to the main joint axis (or parallel), and the other tab offset ran in the transverse direction. Both joints were joined together by a representative composite tube section.

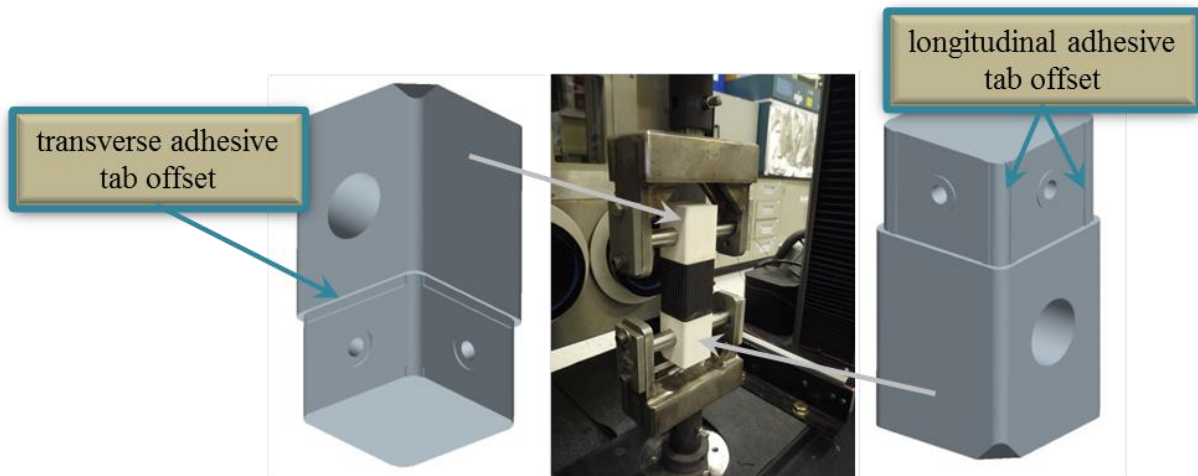


Figure 20. Adhesive joints strength test set-up.

Results of this test sequence are shown in Figure 21 with an approximate ultimate load of 2900 lbf. The longitudinal adhesive offset tab joint began to fail first with a visible dis-bond between the composite tube and the joint where it met the base collar section. Shown in Appendix Figure A4 is the complete plot of the raw data which includes the complete fracturing, or dis-bonding, of the joint. After the ultimate adhesive strength load, the composite section seemed to go into a “Chinese Finger Trap” mode where it shrunk down as more displacement was applied (e.g. became mechanistic in its response relative to Poisson’s effects).

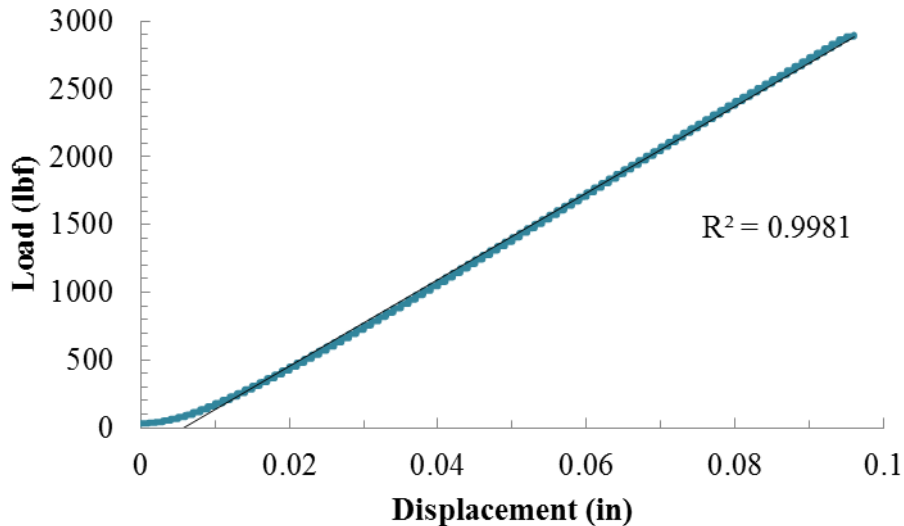
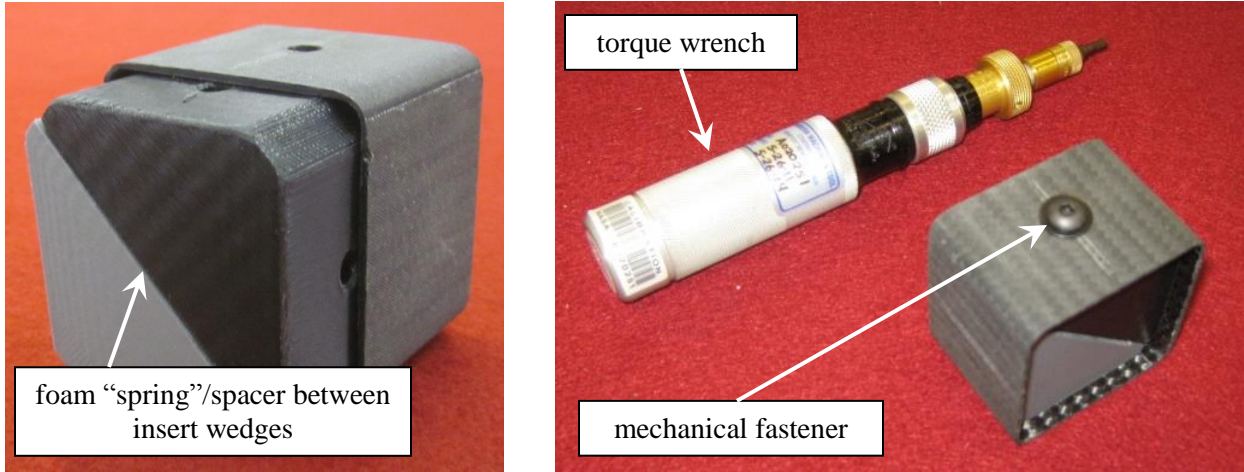


Figure 21. Ultimate joint adhesive layer bond strength test sequence.

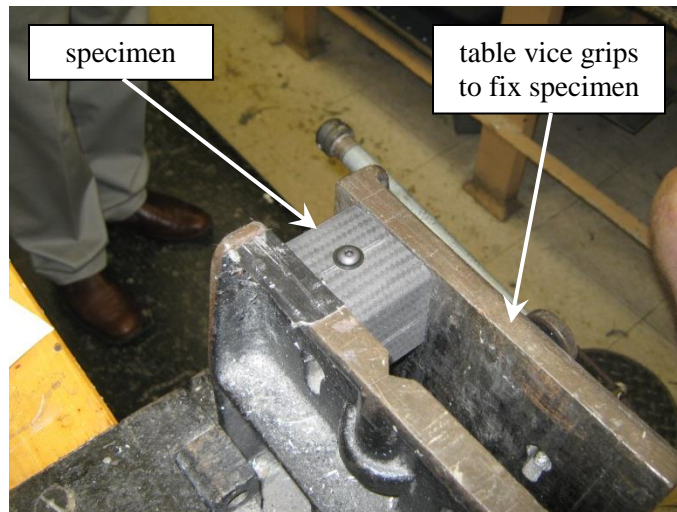
Additionally, baseline torque down tests were conducted to determine the degree to which the mechanical fastener torque down might bear into the underlying composite tube, and to also ascertain how well the tube insert could pick up such loading. Similar, additional torque down tests were conducted to help determine how well the joint mechanical inserts would take similar

loads (picture not shown). Shown in Figure 22 is the test set-up for the tube inserts, and Table 1 presents the results of both tests.



(a) FDM insert with foam spring

(b) torque wrench with installed fastener



(c) torque down test

Figure 22. FDM tube insert torque down testing.

Rotation of Fastener	Tube Inserts (in-lbs)	Joint Inserts (in-lbs)
Hand tight	1-2	2
¼ turn	9	19
½ turn	30	30

Table 1: FDM Tube Inserts and Joints Fastener Torque Tests

The mechanical fastener torque down tests were stopped at ½ of a full fastener head rotation because there was no additional rotation available, without substantially increased torque, and the technicians and engineers involved in the test felt that it conformed to a good tight torqued down connection.

Lessons Learned

As a result of the tooling, and machine expertise needed in traditional manufacturing methods, it was found that the AM method, whereby complex parts are produced in a near net final shape via 3D printing methods, offered potential mass, reusability, and multi-purposing factors not achievable with more traditional methods. This approach offers a substantial advantage for in-situ utilization and repurposing, and manufacturing in space. Initial joint and adhesive bondline strength tests show promise for this approach, and could be expanded to include launch load conditions, and/or modified for in-space assembly conceptual approaches. The braided carbon composite tubes were stiff and were also problematic when it came to drilling thru holes for the mechanical fasteners. The dust generated from the carbon tubes proved to be a skin irritant, and would have to be addressed for in-situ manufacturing.

During the evolution of the CR, and in particular during the joints production phase of the activity, a process was developed whereby sparse fill sections could be created which essentially allowed for a honeycomb type interior structure (i.e. reducing mass, but retaining primary strength in principal load directions). This resulted in significant weight savings while reducing production time and costs. Additionally, it was found that by using a soldering gun to heat up the mechanical fastener inserts for the joints, that they could easily be installed by direct melt-infusion into the pre-fabricated thru hole.

Additionally, while producing the back honeycomb panel clam-shell, it was discovered that the rack was more easily produced if specific facesheet slices were cut and bent (where they interfaced with the horizontal composite tubes), with a subsequent core-out of the honeycomb section, and then that section was attached along all of the tube and joint interfaces. The alternative would have been to have individual rectangular sections for each planar area, which would have required close-out/safety potting at each edge, and so on.

Concluding Remarks

A novel, light weight, and stiff CR rack design was manufactured using AM printed joints, braided carbon composite tubing, and which included both adhesive and mechanical fastening approaches, and which also utilized aircraft grade composite honeycomb panels as walling/flooring. As outlined in the joint/adhesive tests sections, additional research could be conducted which would quantify the joint strengths more, and allow for more of a baseline comparison to legacy ISPRs.

All new novel AM joints, with minimal complexity, as well as novel AM tube inserts were developed during this effort and were shown to have great promise in constructing such prototypes. The strength levels determined during testing could be investigated further to include additional design and manufacturing approaches. Examples would include additional features to

enhance the strength of the adhesive bondline (such as more tabs, or different orientations, or a greater roughening of the part at the adhesive layer interface). Additional investigation into the mechanistic, universal joints concept would also be worthwhile.

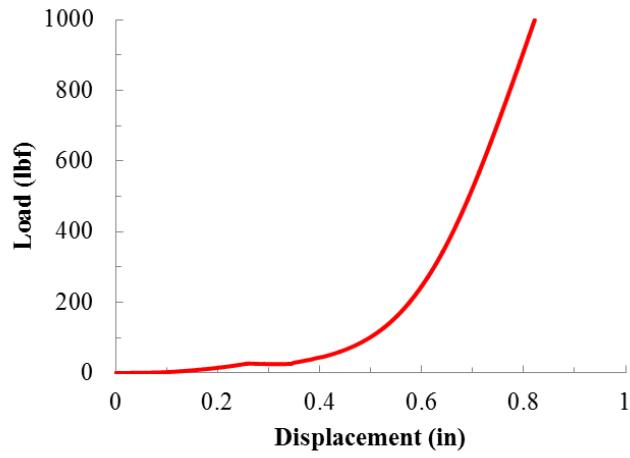
The integrated use of novel manufacturing methods and composites hold great potential for use in spaceflight applications. Such methods need to be explored further for building up secondary interior structures for launch scenarios, as well as for potential in-space assembly. Additionally, the ability to use AM components designed for manufacturing in space opens up more possibilities when outfitting spacecraft interiors and making repairs (or having spare parts, the commonality of which is an issue of concern). However, one should also consider using such methods demonstrated in this composite structure for replacing traditional manufacturing methods (i.e. machined components). Another aspect to consider is that by producing equipment racks that can be disassembled, one could then reconfigure the interior of a spacecraft using the structural components from such a rack.

As outlined this effort produced a minimally reduced volume, as compared to a traditional ISPR, but which utilized SoA approaches to structural joint sections which included 3D printed joints (the AM/FDM methods) and tube inserts, braided square composite tubing and the use of composite honeycomb panels as stress members.

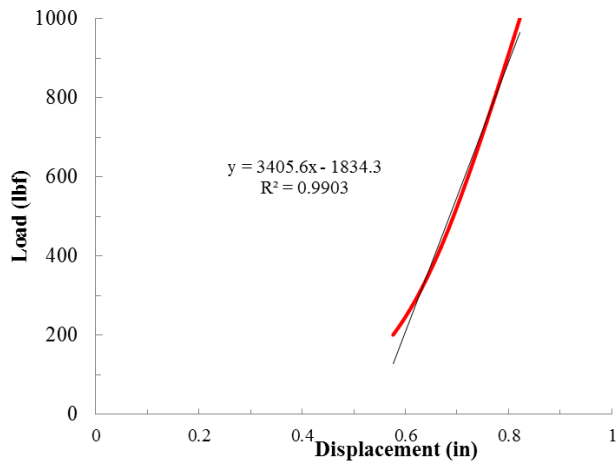
References

1. Smith, Russ; et al: Overview of Evolved Secondary Structural Prototypes with Provisions for Integrated Health Monitoring Sensors in Support of the Deep Space Habitat (forthcoming), 2014.
2. NASA, JSC & Boeing, International Standard Payload Rack (ISPR) Structural Integrator's Handbook. NASA SSP 57007, October 1999.
3. DragonPlate Inc. 2014, Material Specifications, Carbon Fiber Rectangular Tube, <http://dragonplate.com/docs/DPSpecRecTube.pdf>
4. Smith, R.W., Langford, W.M.: Design, Analysis and Fabrication of Secondary Structural Components for the Habitat Demonstration Unit - Deep Space Habitat. Presented at the AIAA-SDM Conference, Honolulu, HI, 23-26 April 2012-#1889.
5. University of Wisconsin, X-Hab 2014, 3D Printer for Space, <http://xhab.engr.wisc.edu/project/>
6. Made In Space Inc. 2014, 3D printer flight experiment & ISS delivery, <http://www.madeinspace.us/projects>
7. Vectorworks 2012 SP5, Designer, Renderworks, etc, Nemetschek Vectorworks Inc.
8. CREO 2.0, PTC Inc. 2013
9. Stratsys Fortus e-V, 2013, Fused Deposition Modeling systems with part processing by Insight, 7665 Commerce Way, Eden Prairie, MN 55344

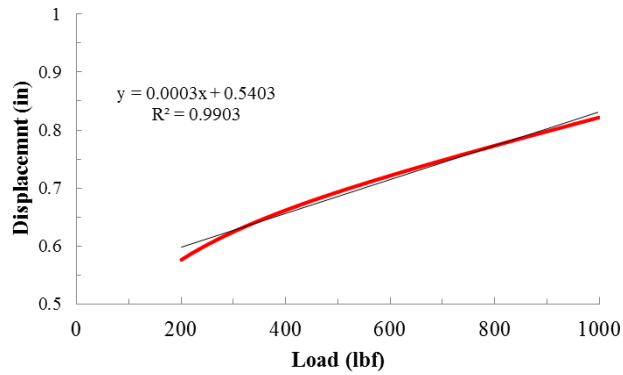
Appendix A: Joint screening tests raw and refined data results



(a) raw load vs. displacement

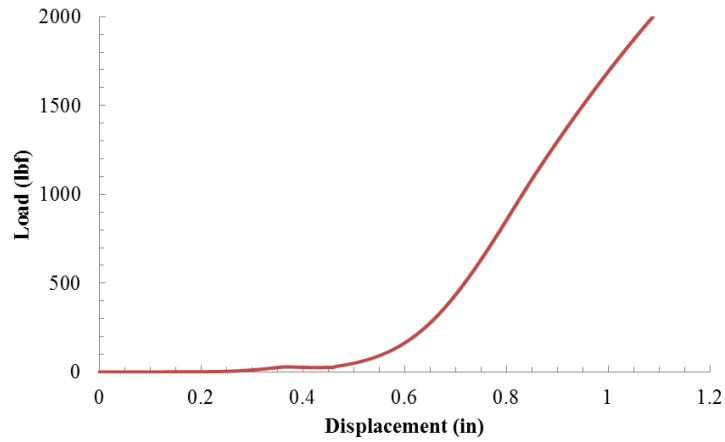


(b) linearized load vs. displacement

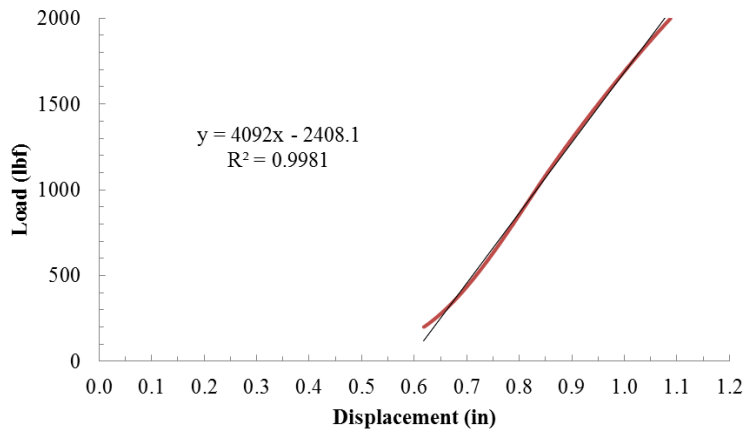


(c) linearized response showing nominal 0.54 inch offset

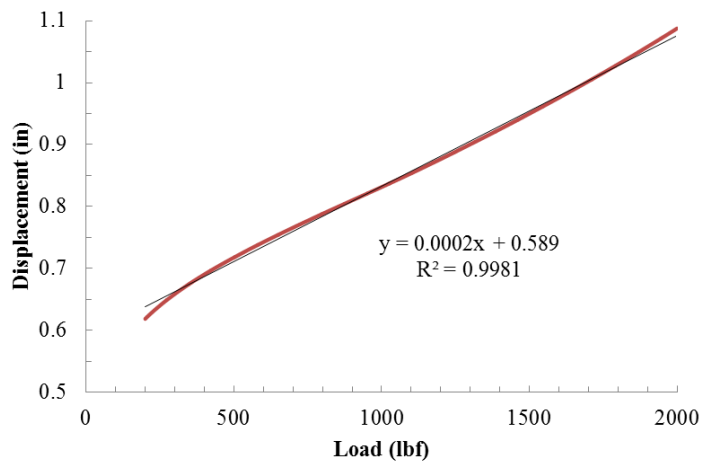
Figure A1. Initial load vs. displacement response for bending tests.



(a) raw load vs. displacement

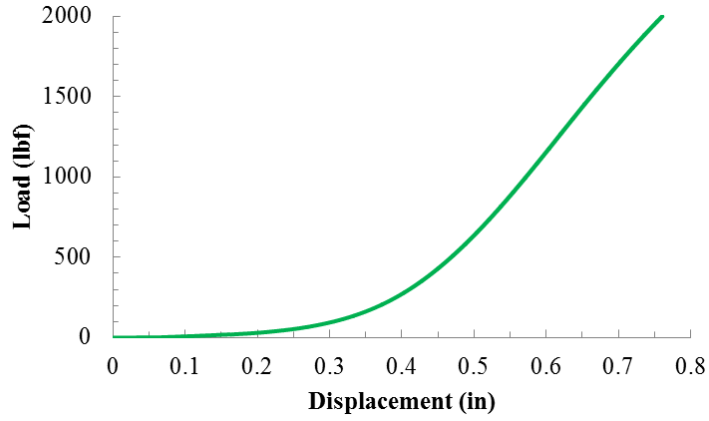


(b) linearized load vs. displacement

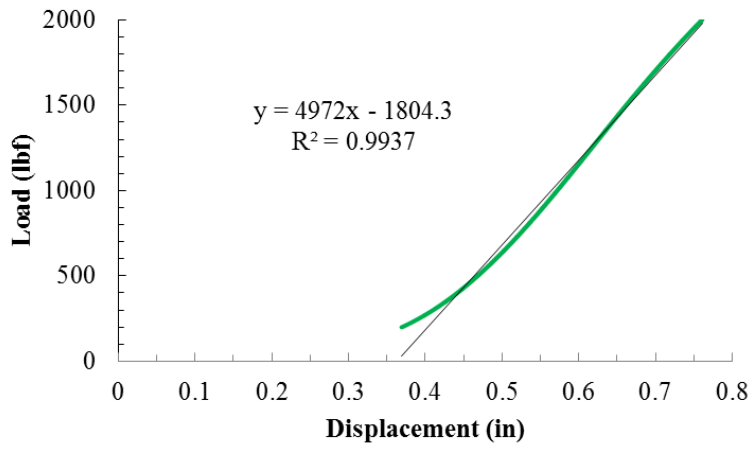


(c) linearized response showing nominal 0.59 inch offset

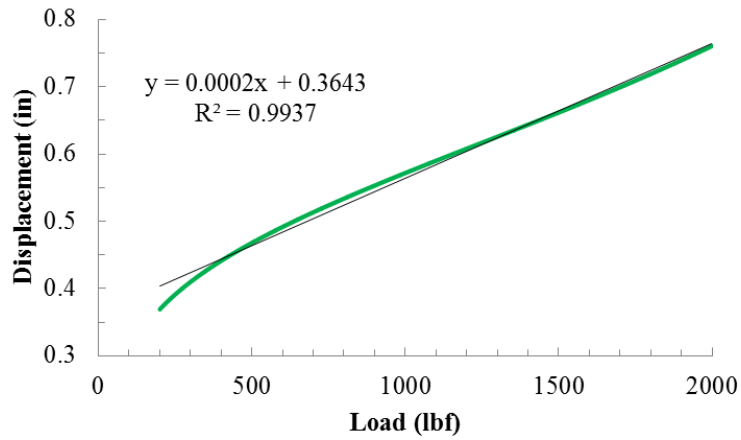
Figure A2. Bending test results for final bending sequence.



(a) raw load vs. displacement



(b) linearized load vs. displacement



(c) linearized response showing nominal 0.36 inch offset

Figure A3. Load vs. displacement response for tensile test.